International Journal of Biochemistry and Cell Biology 109 (2019) 59–68

Contents lists available at ScienceDirect

International Journal of Biochemistry and Cell Biology

journal homepage: www.elsevier.com/locate/biocel

Exosomes from hypoxia-treated human adipose-derived mesenchymal stem cells enhance angiogenesis through VEGF/VEGF-R

Yudi Han[a,b,c], Jing Ren[a,c], Yun Bai[a], Xuetao Pei[d,*], Yan Han[a,c,*]

[a] Department of Plastic and Reconstructive Surgery, First Medical Center of PLA General Hospital, Beijing 100853, P.R. China
[b] Department of Burn and Plastic Surgery, Seventh Medical Center of PLA General Hospital, Beijing 100700, P.R. China
[c] Nankai University School of Medicine, Tianjin 300000, P.R. China
[d] Stem Cell and Regenerative Medicine lab, Institute of Health Service and Transfusion Medicine, AMMS, Beijing 100850, China

ARTICLE INFO

Keywords:
Mesenchymal stem cells (MSCs)
Hypoxia
Exosomes
Angiogenesis
Vascular endothelial growth factor (VEGF)

ABSTRACT

Background: We previously reported that co-transplantation of exosomes from hypoxia-preconditioned adipose mesenchymal stem cells (ADSCs) improves the neoangiogenesis and survival of the grafted tissue. This study aimed to investigate the molecular mechanism of this protective effect.

Methods: Exosomes were collected from normoxia-treated (nADSC-Exo) or hypoxia–treated (hypADSC-Exo) human ADSCs, and their pro-angiogenic capacity was evaluated in human umbilical vein endothelial cells (HUVECs) and a nude mouse model of subcutaneous fat grafting. Protein array was used to compare the exosome-derived proteins between nADSC-Exo and hypADSC-Exo.

Results: Compared with the nADSC-Exo group and untreated control, hypADSC-Exo treatment significantly promoted proliferation, migration and tube-formation capability of HUVECs. Protein array revealed that the levels of vascular endothelial growth factor (VEGF), epidermal growth factor (EGF), fibroblast growth factor (FGF) and their receptors (VEGF-R2, VEGF-R3), and monocyte chemoattractant protein 2 (MCP-2), monocyte chemoattractant protein 4 (MCP-4) were significantly higher in the hypADSC-Exo than in the nADSC-Exo. In the nude mice model of fat grafting, immunofluorescence of CD31 showed that hypADSC-Exo dramatically improved neovascularization around the graft. Furthermore, compared with nADSC-Exo and control groups, co-transplantation of hypADSC-Exo significantly increased the protein expression of EGF, FGF, VEGF/VEGF-R, angiopoietin-1(Ang-1) and tyrosine kinase with immunoglobulin-like and EGF-like domains 1(Tie-1, an angiopoietin receptor) in the grafted tissue at 30 days after transplantation. Immunohistochemical analysis demonstrated that hypADSC-Exo treatment significantly increased VEGF-R expression in the grafted tissue.

Conclusions: Exosomes from hypoxia-treated human ADSCs possess a higher capacity to enhance angiogenesis in fat grafting, at least partially, *via* regulating VEGF/VEGF-R signaling.

1. Introduction

Fat grafting has been widely adopted in aesthetic plastic surgery and reconstruction surgery (Simonacci et al., 2016; Coleman and Katzel, 2015; Condé-Green et al., 2016), however, the survival rate of fat grafts remains unsatisfied (Herold et al., 2013; Wetterau et al., 2012). Due to the low tolerance for ischemia of adipose tissues (Del Vecchio and Del Vecchio, 2014), timely and effective revascularization is crucial for functional recovery in fat grafting and filling (Zhao et al., 2012; Pu, 2016). Co-transplantation of autologous adipose tissue with mesenchymal stem cells (MSCs) can stimulate angiogenesis by secreting multiple angiogenic cytokines and differentiating into endothelial cells (Suga et al., 2014), which is known as the cell-assisted lipotransfer (CAL) technique (Yoshimura et al., 2008a,b). However, a major dilemma in CAL is the low survival of transplanted cells in the ischemic region (Zhao et al., 2012; Comella et al., 2017). Most transplanted cells die in the ischemic region within 4 days posttransplantation (Simonacci et al., 2016). This problem cannot be resolved by simply increasing the

Abbreviations: ADSCs, adipose mesenchymal stem cells; HUVECs, human umbilical vein endothelial cells; VEGF, vascular endothelial growth factor; EGF, epidermal growth factor; FGF, fibroblast growth factor; MCP-2, monocyte chemoattractant protein 2; Ang-1, angiopoietin-1; MSCs, mesenchymal stem cells; CAL, cell-assisted lipotransfer; VEGFRs, VEGF receptors; SFM, serum-free medium; TEM, transmission electron microscopy; NTA, nanoparticle tracking analysis

* Corresponding authors at: Department of Plastic and Reconstructive Surgery, Chinese PLA General Hospital, No. 28 Fuxing Road, Beijing, 100853, PR China.
E-mail addresses: hanyudi_301@foxmail.com (Y. Han), 412539377@qq.com (J. Ren), 326306263@qq.com (Y. Bai), peixt@nic.bmi.ac.cn (X. Pei), 13720086335@163.com (Y. Han).

https://doi.org/10.1016/j.biocel.2019.01.017
Received 22 July 2018; Received in revised form 11 January 2019; Accepted 29 January 2019
Available online 30 January 2019
1357-2725/ © 2019 Published by Elsevier Ltd.

dose of MSCs transplantation as it would further worse oxygen-blood supply and deteriorate the cell survival environment (Condé-Green et al., 2016). Thus, it is required to develop an alternative option for CAL.

Reduced oxygen availability is a common condition in the damaged tissue. Once migrate to hypoxic areas, MSCs can produce a large amount of therapeutic paracrine factors to repair the damaged tissue (Pankajakshan and Agrawal, 2014). Exosomes are cell-producing small extracellular bilayer membrane vesicles (30–200 nm) carrying proteins and RNAs (Krämer-Albers and Hill, 2016; Raposo and Stoorvogel, 2013). Human MSCs can also produce exosomes in the resting state (Lai et al., 2015). Exosomes have been identified as a contributor to the beneficial paracrine effects of MSC therapy (Bang and Thum, 2012). Recent studies have shown that in addition to MSC-secreting cytokines, MSC-derived exosomes can also promote angiogenesis (Hu et al., 2015; Liu et al., 2017; Merino-González et al., 2016).

It is well established that hypoxia can activate hypoxia-inducible factor (HIF-1α) which regulates transcription of angiogenic genes, such as vascular endothelial growth factor (VEGF), VEGF receptors (VEGFRs), to promote angiogenesis (Majmundar et al., 2010). Accumulating evidence has demonstrated that hypoxia treatment induces MSC production of various therapeutic paracrine factors (Madrigal et al., 2014; Chang et al., 2013). As the cargos carried by exosome are considerably influenced by the microenvironment where the host cells stay (Hofmann et al., 2012), hypoxia preconditioning for MSCs can be used to elevate the levels of paracrine factors in the MSC-derived exosomes. Zhang et al. have demonstrated that hypoxia can enhance the capacity of MSCs-derived microvesicles to promote *in vitro* angiogenesis and blood flow recovery in rat (Zhang et al., 2012). Our previous study also found that hypoxia treatment can significantly elevate the beneficial effect of exosomes in the fat grafting (Han et al., 2018). Co-transplantation of exosomes (hypADSC-Exo) from hypoxia-preconditioned adipose mesenchymal stem cells (ADSCs) improves the blood perfusion and survival of the grafted tissue, as well as attenuates infiltration of inflammatory cells in the nude mice model of fat grafting (Han et al., 2018). These results suggest that hypADSC-Exo can effectively promote neovascularization and graft survival in fat grafting. However, the mechanism underlying the beneficial effect of ADSC-Exos remains to be further elucidated. Therefore, the purpose of the current study was to elucidate the molecular mechanism of the protective effect of hypADSC-Exo.

2. Materials and methods

2.1. Cell culture and hypoxia protocol

Human adipose tissues were obtained from patients undergoing tumescent liposuctions with informed consent and all experiments were approved by the Ethics Committee at the Chinese PLA General Hospital, and all clinical investigations were conducted according to the principles expressed in the Declaration of Helsinki. Human ADSCs were isolated from human adipose tissues and characterized as previously described (Han et al., 2018). After isolation, ADSCs were maintained in a serum-free medium (SFM) specially formulated for the growth and expansion of human mesenchymal stem cells (CTS™ StemPro™ MSC SFM, Gibco, USA). Passage 3 ADSCs were used in the experiments.

For exosome isolation, ADSCs were seeded at a density of 5×10^3 cells/cm^2 and cultured in the complete α-MEM medium until 70–80% confluence. The cells were cultured for an additional 48 h under hypoxia or normoxia in serum-free α-MEM medium. The conditioned medium was collected for exosome isolation. Hypoxia treatment was carried out using a tri-gas incubator. The oxygen concentration was maintained at 5% with a residual gas mixture composed of 5% CO_2 and balanced nitrogen.

Human umbilical vein endothelial cells (HUVECs) were prepared and cultured as routinely described (Cheung, 2007). In brief, umbilical cord was collected from Department of gynecology and obstetrics, PLA general hospital with informed consent. The umbilical veins were isolated and washed twice with PBS, followed by digestion with 0.1% collagen P (Sigma, USA) for 15 min at 37 °C. The endothelial cells were then flushed out. HUVECs were seeded onto 0.1% gelatin-coated plastic dishes, maintained in endothelial growth medium-2 (EGM-2, Lonza, USA) and starved in EBM-2 containing 0.5% fetal bovine serum overnight before cell assays were performed.

2.2. Exosome harvest and identification

Exosome purification was performed according to differential centrifugation approach (Théry et al., 2006). Briefly, ADSCs culture medium was collected and centrifuged at 1500 × *g* for 5 min and then for an additional 5 min at 3000 × *g* to remove cell debris. Then the supernatant was filtered through a 0.22-μm pore membrane filter (Millipore, USA) to remove large membrane vesicles, followed by ultracentrifugation at 100,000 × *g*, 4 °C for 90 min. The pellet was resuspended in 1 mL sterile/filtered PBS, followed by centrifuged at 100,000 × *g* for 60 min and resuspended in 100 μL PBS. Exosomes were either used immediately (on ice) or stored at −80 °C. The protein concentration of the exosomes was determined using the Bradford protein assay according to the manufacturer's protocol (Bio-Rad, USA). The exosome morphologies were characterized using 100 kv transmission electron microscopy (TEM, HITACHI H-7000FA, Japan). The exosomal surface marker proteins including CD9, TSG101 and CD63 was analyzed by FACS analysis with vesicles pre-absorbed on latex beads (4% polystyrene latex beads, ThermoFisher, USA). The bead- exosome aggregates were labeled with different fluorescence-labeled antibodies, including anti-CD9 (1:200, eBioscience, USA), anti-TSG101 (1:200 eBioscience), anti-CD63 (1:200 eBioscience) and MSC-related surface marker antibodies, including anti-CD90 (1:200 eBioscience) and anti-CD34 (1:200 eBioscience). The particle size, concentration, and video frame of exosomes were analyzed by using nanoparticle tracking analysis (NTA) system (LM10 NanoSight, USA) and Nanoparticle Tracking Analysis software (version2.2 NanoSight).

2.3. Internalization of exosome into HUVECs

Human ADSCs-Exos were labeled with PKH26 dye (Sigma Aldrich, USA), followed by filtered through a 10-kDa filter (Microcon YM-100, Millipore, USA) and resuspended in PBS for 3 times to remove excessive dye. HUVECs were incubated with the labeled exosomes in serum-free medium at 37 °C overnight. After fixed with 4% paraformaldehyde (PFA) and stained with 4′, 6-diamidino-2-phenylindole (DAPI, Sigma, USA), the cells were observed under an Eclipse Ti-S fluorescence microscope (Nikon, Japan).

2.4. Cell proliferation assay

A Cell Counting Kit-8 assay (CCK-8; Dojindo) was used to assess cell proliferation. HUVECs were seeded onto 96-well plates (5×10^3 cells/well) and cultured in serum-free EBM-2 medium containing 50 μg/ml Hypoxic ADSC-Exo or 50 μg/ml ADSC-Exo or an equal volume of PBS. At 0, 6, 12, 24, and 48 h, the CCK-8 solution was added to HUVECs (10 μL per well) and cells were incubated at 37 ℃ for 2 h. The absorbance was measured at 450 nm by using a microplate reader and the optical density values represented the survival/proliferation of HUVECs.

2.5. Cell migration assay

HUVECs were plated in 12-well plates (2×10^5 cells/well) and incubated at 37 ℃ until 90% confluence. The confluent monolayer was scratched using a 200 μl pipette tip and washed with PBS to remove the debris and smooth the edge of the scratch. The serum-free EBM-2

medium (500 μl) with exosomes (50 μg/ml nADSC-Exo or hypADSC-Exo) or PBS was added to the well. Cells were photographed immediately (t = 0 h), 6 h and 12 h later. The level of migration was measured by the ratio of closure area to initial wound area (t = 0 h) as follows: migration area (%) = (A0 – An)/A0 × 100, where A0 represents the area of initial wound area, An represents the residual area of wound at the metering point (t = n h).

2.6. Transwell migration assay

For the transwell migration assay, HUVECs (1 × 105 cells/well, three replicates per group) were seeded onto upper chambers of transwell 24-well plates (Corning, Corning, NY, USA) with 8 μm pore filters containing serum-containing (5%) EBM-2 medium and cultured for 12 h. Then the lower chamber was replaced with serum-free EBM-2 medium supplemented with or without nADSC-Exos (50 μg/well) or hypADSC-Exos (50 μg/well). After 12 h, the cells attached on the upper surface of the filter membranes were cleaned by a cotton swab, the cells at the bottom of the membrane were fixed with 4% paraformaldehyde and then stained by 0.5% crystal violet (Sigma Aldrich, St. Louis, MO, USA) to visualize the migrated cells under an optical microscope (Leica DMI6000B, Germany). Three fields from each well were randomly selected for quantitatively determining the color-positive area using Image-Pro Plus 6.0 software (Media Cybernetics, Rockville, MD, USA).

2.7. Tube formation assay

Aliquots of HUVECs (5×10^4) were seeded onto growth factor reduced Matrigel (No. 354230, BD, USA) coated wells of a 48-well plate and cultured in 1% FBS-supplemented EBM-2 in the presence of nADSC-Exo or hypADSC-Exo at the indicated concentrations (50 μg/ml) for 12 h. Triple wells were set for each concentration. Tube formation was examined by a phase-contrast microscopy (Olympus, Tokyo, Japan), and the tube length was measured as the mean summed length of capillary-like structures (> 6 cell long) per well, per high-power field using ImageJ software (NIH, USA).

2.8. Animal model of fat grafts angiogenesis

Six-week-old, female, BALB/c nude mice were obtained from the Laboratory Animal Center of PLA General Hospital (Beijing, China). All experimental and animal care procedures were approved by the Animal Care and Use Committee of Chinese PLA General Hospital and performed in accordance with the National Institutes of Health Guidelines for the Care and Use of Laboratory Animals. After one week of acclimation, the mice were anesthetized with intramuscular injections of pentobarbital (1%, 50 mg/kg). Three points were selected from the mouse back, then, the aspirated human fat sample (1 ml for each point) was injected subcutaneously using a 2.5-ml injection syringe (Zhao et al., 2012). The human adipose tissue was obtained from a female patient receiving an abdominal liposuction bariatric surgery with informed consent.

In the control group, the fat sample was injected with 100 μl of sterile phosphate-buffered saline (PBS). In exosomes-treated groups, mice were injected with either nADSC-Exo (50 μg/100 μl) or hypADSC-Exo (50 μg/100 μl). The same supplementary injections were performed regularly at 1-week intervals after the first injection. After 2 days (n = 5), 15 days (n = 5), and 30 days (n = 5) following grafting, the mice were sacrificed, and the grafted sample was collected for histologically examined.

2.9. Real-Time PCR

Total RNA was extracted from HUVECs using Trizol reagent (Sigma, USA), followed by reversely transcribed to generate the first strand cDNA using a reverse transcription system (Takara, Japan) according to manufacturer's protocol. Quantitative PCR was performed using the SYBR Green PCR mix (Toyobo, Japan) on a Bio-Rad CFX Connect real-time system (Bio-Rad, USA). The primers were as follows: *Ang-1* (forward primer: GGGGGAGGTTGGACTGTAAT; reverse primer: GAATAG GCTCGGTTCCCTTC) and *Tie-1* (forward primer: GACTGACCCAGCTTT TGCTC; reverse primer: CTGCAATCTTGGAGGCTAGG), and *GAPDH* (forward primer: GAGTCAACGGATTTGGTCGT; reverse primer: TTGA TTTTGGAGGGATCTCG). *GAPDH* was used as an internal control to normalize for differences in the amount of total RNA in each sample.

2.10. Human growth factor antibody array

Human growth factors were analyzed by using a Human Growth Factor Antibody Array (GSH-ANG-3, RayBiotech, USA) according to the manufacturer's instructions to measure the expression levels of 30 growth factors. Positive signals were captured on glass chips using a laser scanner (GenePix 4000B Microarray Scanner; Molecular Devices, Sunnyvale, CA, USA) and analyzed with GenePix Pro 6.0. The observed fluorescence intensities were normalized to the intensities of the internal positive controls.

2.11. Western blot

Western blot was performed as previously described (Guo et al., 2017). In brief, exosomes, cells, or tissue were lysed in RIPA buffer. The protein samples were electrophoresed by using 12% SDS gels, and then transferred onto polyvinylidene fluoride membranes (EMD Millipore, USA). Then, the membranes were incubated with the monoclonal primary antibodies overnight as follows: CD63 (1:1000, Cell Signaling, USA), CD9 (1:1000, Proteintech, USA), TSG101 (1:1000, Proteintech), vascular endothelial growth factor A (VEGF-A) (1:1000, Abcam, USA) vascular endothelial growth factor Receptor2 (VEGF-R2) (1:1000, Proteintech). Subsequently, horseradish peroxidase (HRP)-conjugated anti-rabbit or anti-mouse IgG (1:2000, ZSGB-BIO, USA) secondary antibody was added at room temperature for 1 h. The target proteins were visualized using the ECL (EMD Millipore). Densitometric analysis for the quantification of the bands was performed using Quantity One software (Bio-Rad Laboratories, USA).

2.12. Histological examination

To quantitatively determine the vessels in the tissue section, immunofluorescence staining for CD31 was performed. After fixation with paraformaldehyde and dehydration with sucrose, tissues were embedded in OCT. A 5-μm-thick section was blocked with 1.5% goat serum and incubated with primary antibodies against the vascular endothelial marker CD31 (1:500, Abcam) overnight at 4 °C, followed by incubated with Alexa Fluor 488- and Cy3-conjugated secondary antibodies and 4′,6-diamidino-2-phenylindole (DAPI, Sigma-Aldrich) to stain the nuclei. The images were examined with an LSM-880 confocal microscope (Carl Zeiss, Oberkochen, Germany).

For immunohistochemical staining for VEGF-R, sections were deparaffinized and rehydrated through a graded series of ethanol washes, then blocked with a serum-free protein block (Invitrogen). Samples were then incubated with rabbit anti-human VEGF-R antibody (1:200, Proteintech) at 4 °C overnight. Samples were incubated in biotinylated goat anti-rabbit IgG antibody (Invitrogen) at room temperature for 1 h, followed by development with 3,3-diaminobenzidine tetrahydrochloride (DAB; DAKO, Japan). Three fields from each tissue section were randomly selected and quantitatively determined the positive signal using Image-Pro Plus 6.0 software (Media Cybernetics, Rockville, MD, USA) by measuring the mean density (IOD/area).

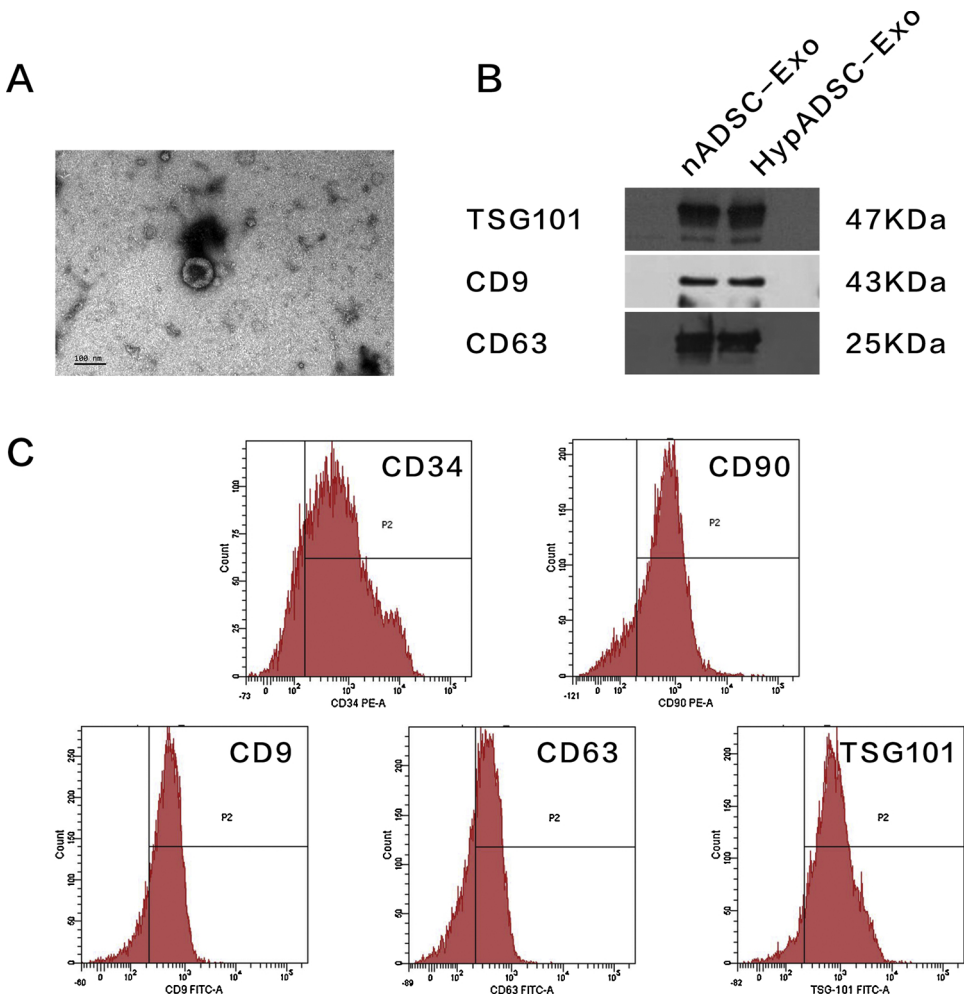

Fig. 1. Characterization of ADSC-Exo. (A) Representative TEM image of ADSC-Exo. (B) Western blot analysis of the exosomal markers (TSG101, CD9, and CD63). (C) Flow cytometry analysis of exosomal marker (CD9, CD63, TSG101) and MSC-related surface marker (CD90, CD34).

2.13. Statistical analysis

Statistical analysis was performed using GraphPad Prism 5 (GraphPad, USA) and SPSS 17.0 (IBM Corporation, USA). All data are presented as the means ± standard errors from at least 3 independent experiments. Individual data in experimental groups were compared using the Student t-test. Comparison among groups was performed by one-way ANOVA with Tukey's HSD test post-hoc comparisons. A $P < 0.05$ was considered statistically significant.

3. Results

3.1. Characterization of exosomes derived from normoxia and hypoxic ADSCs

Exosomes were collected from ADSC conditioned medium in normoxia condition (nADSC-Exo) or 5% O_2 hypoxia (hypADSC-Exo). The transmission electron microscopy showed classic cup-shaped morphology and small vesicle structure of exosomes (Fig. 1A). Western blot analysis (Fig. 1B) and flow cytometry (Fig. 1C) demonstrated that these vesicles displayed exosomal surface markers (CD9, CD63, TSG101) and MSC-related surface markers (CD90, CD34). Nanoparticle tracking analysis (NTA) showed the mean sizes of nADSC-Exo and hypADSC-Exo were 75 ± 61 nm and 130 ± 65 nm, respectively (Fig. 2). The mode size of vesicles was also different between nADSC-Exo and hypADSC-Exo. There were three peaks (22, 58, 97 nm) in the mode size of nADSC-Exo. While in the hypADSC-Exo, the mode size focused on a larger peak around 76 and 94 nm, with an increased curve area (Fig. 2). This result suggested that hypoxia treatment caused ADSCs produced larger vesicles.

3.2. ADSC-derived exosomes can be transferred to human umbilical vein endothelial cells (HUVECs)

Exosomes can be internalized by other cells (Tian et al., 2013). To monitor exosome traffic, exosomes were labeled with a PKH26 red fluorescent dye. As shown in Fig. 3, after 6 h incubation with PKH26-labelled ADSC-Exo, red fluorescence spots were scattered and a small amount of fluorescence was observed around the nucleus of HUVECs. At 12 h, stronger red fluorescence gathered around the nucleus of HUVECs (Fig. 3). These results indicated that ADSC-Exo can be gradually internalized by HUVECs.

3.3. Hypoxic ADSC-Exo promoted biological functions of HUVECs in vitro

To investigate the mechanism of enhancing effect of ADSC-Exos cotransplantation on the survival of graft in fat grafting, we first assessed the effect of exosome derived from hypoxia-treated ADSCs on the biological functions of HUVECs. CCK8 assay showed that compared with the control group, hypADSC-Exo (50 μg/mL) significantly promoted proliferation of HUVECs ($P < 0.05$ at 12–48 h, Fig. 4A).The proliferation enhancing effect peaked at 12 h and subsequently plateaued.

To test the effect of ADSC-Exo on HUVECs migration, scratch test

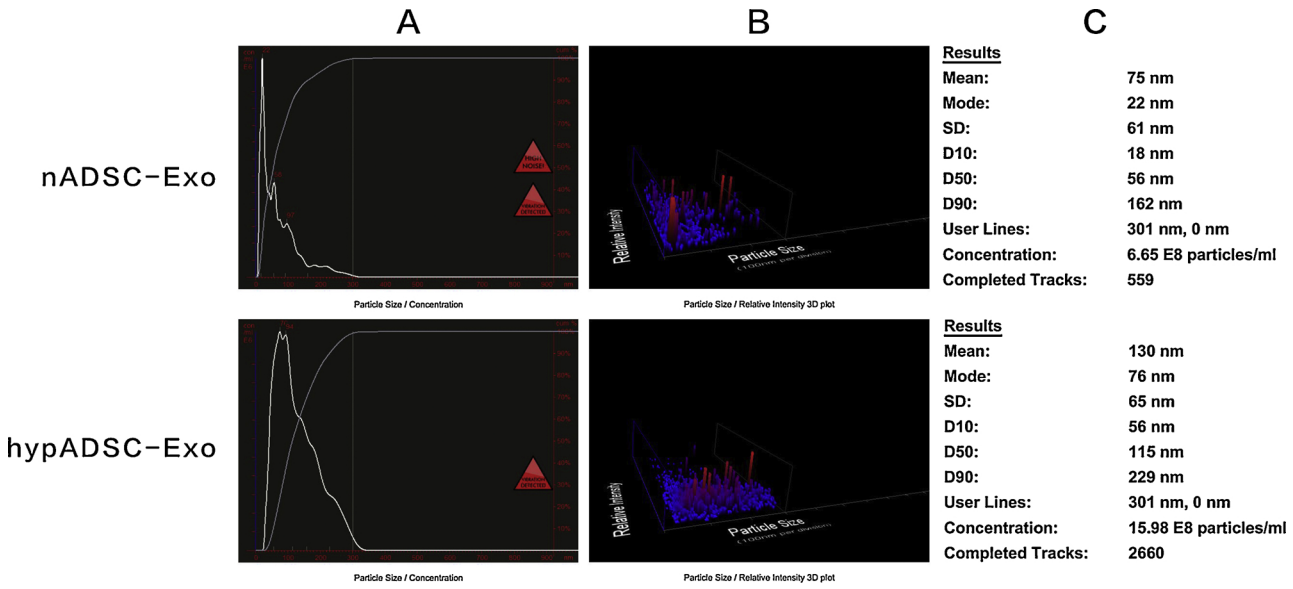

Fig. 2. The size of exosomes was measured by NanoSight analysis. (A) The curves showed the particle size distribution of nADSC-Exo and hypADSC-Exo. The x-coordinate represents the particle diameter. (B) Size distribution in three dimensions. (C) Concentration analysis of nADSC-Exo and hypADSC-Exo. The mean diameter and other parameters were shown.

assay was employed. As shown in Fig. 4B, hypADSC-Exo significantly enhanced migration of HUVECs as compared with nADSC-Exo and control groups ($P < 0.05$ at both 6 h and 12 h, Fig. 4B and C). The migration-promoting effect of hypADSC-Exos was further confirmed by the transwell migration assay. As shown in Fig. 4D and E, nADSC-exosomes treatment for 12 h significantly enhanced migratory capacity of HUVEC cells. Moreover, the migratory capacity of HUVECs was significantly greater than in the hypADSC-Exo group than in the nADSC-Exos group. This result indicated that hypADSC-Exo remarkably up-regulated the migration capacity of HUVECs.

Next, the effect of ADSC-Exo on tube-formation capability was evaluated by the *in-vitro* matrigel system. Microscopic observation found that ADSC-Exo treatment promoted tube-like formation of HUVECs at 6 h, and the number of tube-like structure peaked at 12 h (Fig. 4D). Quantitative analysis indicated that hypADSC-Exo significantly promoted tube-like formation at 6 h as compared with nADSC-Exo ($p < 0.05$, Fig. 4E). In addition, qRT-PCR data also suggested the mRNA expressions of angiopoietin-1(*Ang-1*) and tyrosine kinase with immunoglobulin-like and EGF-like domains 1(*Tie-1,* an angiopoietin receptor) were significantly elevated in the hypADSC-Exo group than in the nADSC-Exo group or negative control (all $p < 0.05$, Fig. 4F).

Taken together, these data indicated that ADSC-Exo promoted the proliferation, migration and tube-formation capability of HUVECs, and hypoxia treatment can further elevate the enhancing effects.

3.4. Hypoxia preconditioning elevated the levels of angiogenic proteins in ADSC-Exo

To compare the exosome-derived proteins between nADSC-Exo and

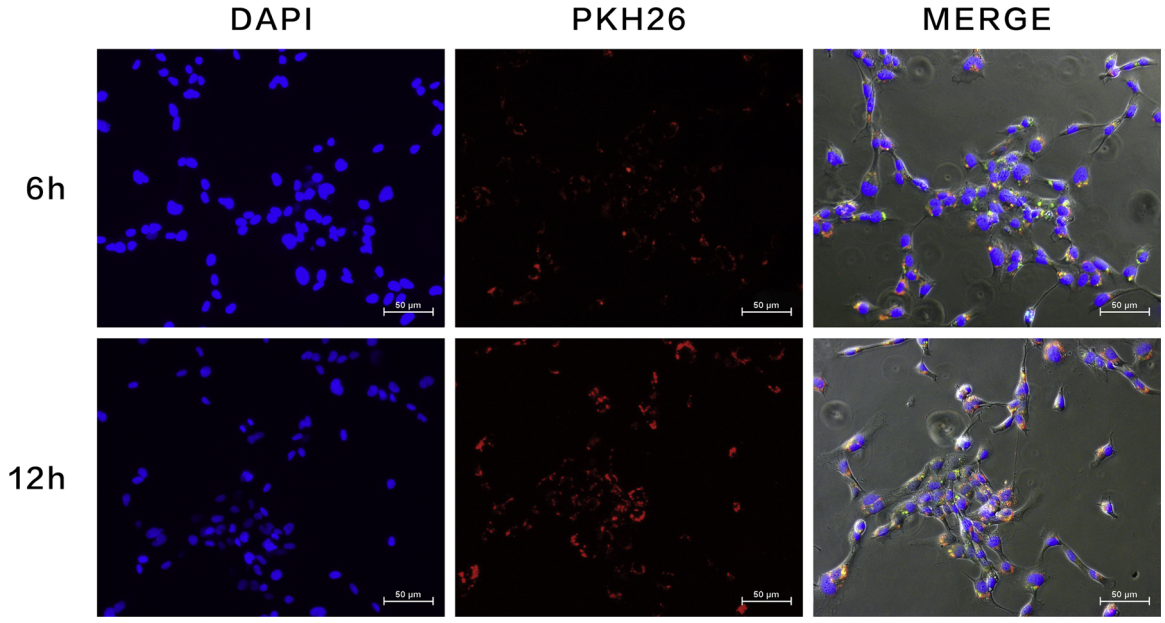

Fig. 3. Dynamic tracking of ADSC-Exo internalization by HUVECs. ADSC-Exo, HUVECs (nuclei stained with DAPI) incubated with ADSC-Exo (labeled with PKH26 dye, red) for 6 and 12 h. Representative fluorescence images were shown.

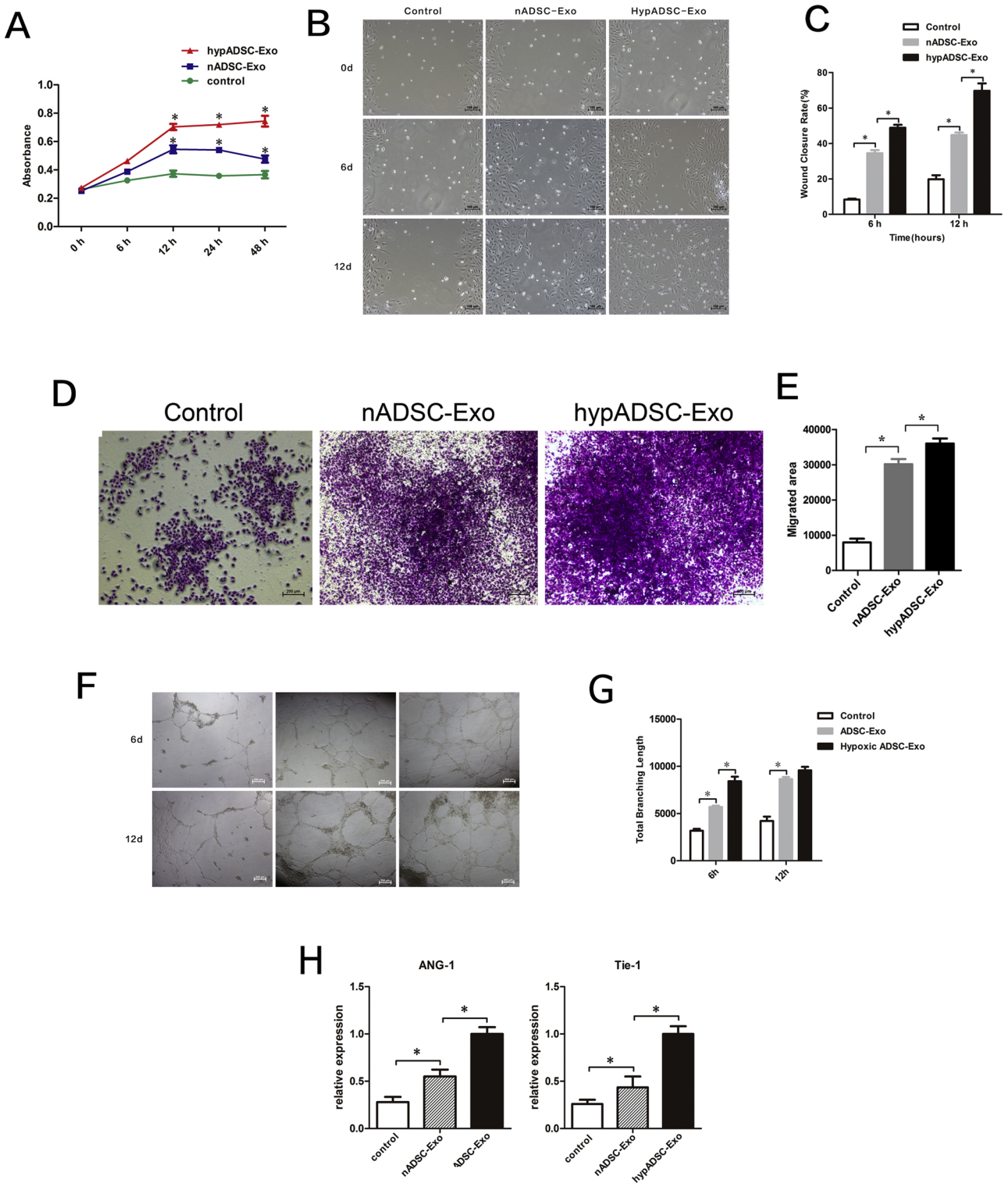

Fig. 4. HypADSC-Exo enhanced the angiogenic capacity of HUVECs *in vitro*. (A) Diagram of HUVECs proliferation in response to nADSC-Exo or hypADSC-Exo; serum-free medium was used as the untreated control (mean ± SEM, * $p < 0.05$ *vs.* untreated control HUVECs, n = 5). (B) The images of scratch test assay in HUVECs. Cells were scratched, photographed at time 0, and incubated in the presence of nADSC-Exo or hypADSC-Exo. Photographs were taken again after 6 h and 12 h. (C) Quantification of the closure area was presented as the ratio of closure area to the initial wound area. The diagram illustrates the mean ± SEM of 3 independent experiments (*$P < 0.05$). (D) Representative image of the transwell assay. HUVECs on the upper side of the transwell membrane were treated with or without nADSC-Exos (50 μg/well) or hypADSC-Exos (50 μg/well) in the lower side for 12 h. The cells migrated to the bottom of the membrane were fixed with 4% paraformaldehyde and stained with crystal violet. Scale bar: 200 μm. (E) Quantitative analysis of the migrated cells (mean ± SEM, * $p < 0.05$, n = 3). (F) Tube-like structures formation by HMECs with nADSC-Exo or hypADSC-Exo stimulation was observed at 6 h and 12 h. (G) Quantitative analysis of tube-like structures formation in response to nADSC-Exo and hypADSC-Exo (mean ± SEM, * $p < 0.05$, n = 3). (H) mRNA expressions of angiopoietin-1(Ang-1) and tyrosine kinase with immunoglobulin-like and EGF-like domains 1(Tie-1) in HUVECs treated with nADSC-Exo or hypADSC-Exo. Serum-free medium was used as negative control (mean ± SEM, * $p < 0.05$, n = 3).

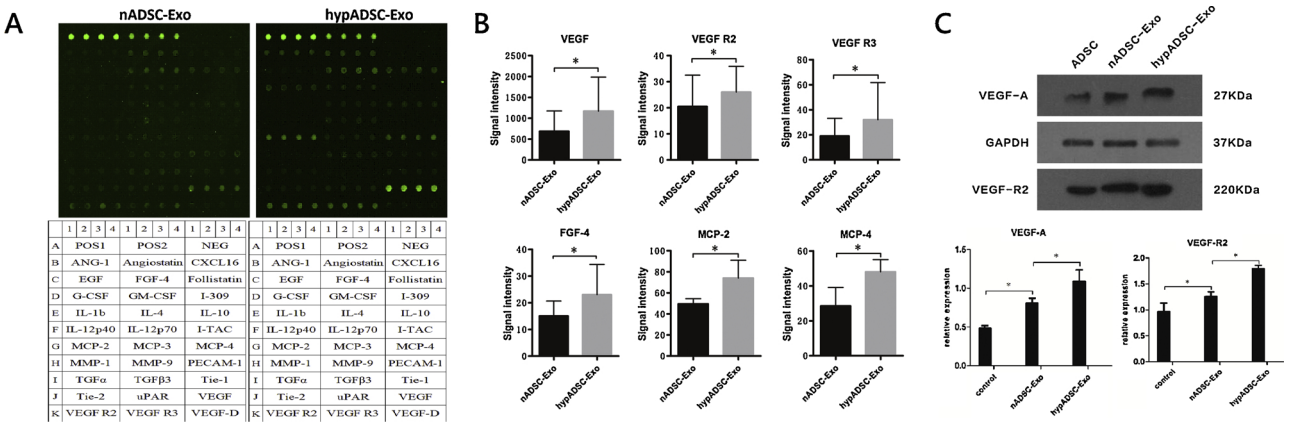

	1	2	3	4	1	2	3	4	1	2	3	4
A	POS1				POS2				NEG			
B	ANG-1				Angiostatin				CXCL16			
C	EGF				FGF-4				Follistatin			
D	G-CSF				GM-CSF				I-309			
E	IL-1b				IL-4				IL-10			
F	IL-12p40				IL-12p70				I-TAC			
G	MCP-2				MCP-3				MCP-4			
H	MMP-1				MMP-9				PECAM-1			
I	TGFα				TGFβ3				Tie-1			
J	Tie-2				uPAR				VEGF			
K	VEGF R2				VEGF R3				VEGF-D			

	1	2	3	4	1	2	3	4	1	2	3	4
A	POS1				POS2				NEG			
B	ANG-1				Angiostatin				CXCL16			
C	EGF				FGF-4				Follistatin			
D	G-CSF				GM-CSF				I-309			
E	IL-1b				IL-4				IL-10			
F	IL-12p40				IL-12p70				I-TAC			
G	MCP-2				MCP-3				MCP-4			
H	MMP-1				MMP-9				PECAM-1			
I	TGFα				TGFβ3				Tie-1			
J	Tie-2				uPAR				VEGF			
K	VEGF R2				VEGF R3				VEGF-D			

Fig. 5. The differential levels of proteins between nADSC-Exo and hypADSC-Exo. (A) The images of the scanned protein array of two groups. The lower table indicates the array map. Each antibody is printed in quadruplicate horizontally. (B) The profiles of proteins that differed between nADSC-Exo and hypADSC-Exo were analyzed by protein array. The image is representative of 2 experiments (*$P < 0.05$). (C) Protein levels of VEGF-A and VEGF-R2 in nADSC-Exo and hypADSC-Exo were detected by Western blotting Analysis (n = 3, *$P < 0.05$).

hypADSC-Exo, protein array for 30 proteins about angiogenic proteins was used (Fig. 5A). The result indicated that exosomes from both normal and hypoxic ADSC contained these 30 proteins (Fig. 5A). However, several proteins were significantly up-regulated in hypADSC-Exo, such as growth factors (vascular endothelial growth factor [VEGF], epidermal growth factor [EGF], fibroblast growth factor [FGF]) and their receptors (VEGF-R2, VEGF-R3), and chemokines (monocyte chemoattractant protein 2 [MCP-2], monocyte chemoattractant protein 4 [MCP-4]) (Fig. 5B). This result demonstrated that hypoxia treatment can elevate the levels of various growth factors associated with angiogenesis in the exosomes. The trends of VEGF-A and VEGF-R2 levels in nADSC-Exo and hypADSC-Exo was confirmed by Western blot analysis (all $P < 0.05$, Fig. 5C).

3.5. ADSC-Exo promoted neovascularization in the nude mice model of fat grafting

To further assess the proangiogenic potential of ADSC-Exo, a nude mice model of fat grafting was adopted. The immunofluorescence of CD31 was used to label the vascular endothelial cells in the tissue around the graft. The results showed that hypADSC-Exo dramatically improved neovascularization as compared with nADSC-Exo and the control groups (Fig. 6A and B), indicated a better proangiogenic potential of hypADSC-Exo.

Histological examination showed that 2 days after grafting, inflammatory cells infiltration and oil cysts formation could be observed in the control mice (Fig. 6C). At 15 days, infiltration of inflammatory cells and necrotic tissues were found in the control mice (Fig. 6C). However, in the nADSC-Exo and hypADSC-Exo-treated mice, these pathological changes could not be found until 30 days (Fig. 6C). Furthermore, the degree of necrosis seemed to be considerably lighter.

3.6. VEGF/VEGF-R were involved in hypADSC-Exo-mediated angiogenesis in vivo

Since ADSC-Exo contained 30 angiogenic proteins, we also assessed the levels of these proteins in the grafted tissue at 30 days after transplantation (Fig. 6D). Protein array showed that the expression of EGF, FGF, VEGF/VEGF-R, and ANG-1/Tie-2 were significantly increased in the hypADSC-Exo group as compared with nADSC-Exo and control groups (all $P < 0.05$, Fig. 6E).

Immunohistochemical analysis for VEGF-R in the grafted fat sample demonstrated that the expression of VEGF-R was detected at 2 days, and was enhanced over time by nADSC-Exo and hypADSC-Exo treatment (all $P < 0.05$, Fig. 6C and F). In addition, hypADSC-Exo significantly increased VEGF-R expression as compared with nADSC-Exo ($P < 0.05$, Fig. 6F).

4. Discussion

In this study, we investigated the molecular mechanism of the protective effect of hypADSC-Exo. The results showed that compared with the nADSC-Exo group and untreated control, hypADSC-Exo treatment significantly promoted proliferation, migration and tube-formation capability of HUVECs. qRT-PCR data demonstrated that hypADSC-Exo up-regulated mRNA expressions of *Ang-1* and *Tie-1* in HUVECs. Protein array revealed that there were significantly higher levels of VEGF, EGF, FGF, VEGF-R2, VEGF-R3, MCP-2, MCP-4 in the hypADSC-Exo than in the nADSC-Exo. In the nude mice model of fat grafting, immunofluorescence of CD31 showed that hypADSC-Exo dramatically improved neovascularization around the graft. HypADSC-Exo treatment attenuated infiltration of inflammatory cells and necrosis in the grafted tissue of mice. Furthermore, cotransplantation of hypADSC-Exo significantly increased the protein expression of EGF, FGF, VEGF/VEGF-R, and ANG-1/Tie-2 in the grafted tissue at 30 days after transplantation. IHC analysis demonstrated that hypADSC-Exo treatment significantly increased VEGF-R protein level in the grafted tissue. Taken together, these findings suggested that exosomes from hypoxia-treated human ADSCs can enhance neovascularization in fat grafting through VEGF/VEGF-R signaling.

In this study, hypADSC-Exo showed superior effects to nADSC-Exo in terms of proliferation, migration, tube formation, and angiogenesis-related mRNA expressions in HUVECs. Notably, we found that the proliferation of HUVECs peaked at 12 h, suggesting that the effect of ADSC-Exo was temporary and expired after 12 h. One possible explanation might be that the angiogenic proteins encapsulated within the exosome was exposed and exerted its effects during the exosome–cytomembrane interaction. After being endocytosed and degraded by target cells, the enhancing effect of angiogenic proteins was diminished. However, further study is necessary to elucidate the mechanism of this phenomenon.

Adipose tissue is highly vascularized, and revascularization at the early stage is crucial for the survival of grafted fat (Stillaert et al., 2016). In the current study, ADSC-Exo enhanced neoangiogenesis in the grafted tissue of mice. Since we observed that PKH26-labelled ADSC-Exo can be gradually internalized by HUVECs, ADSC-Exo may exert its pro-angiogenic function by penetration into the vascular endothelial cells and pericytes in the grafted fat granules. Our results demonstrated that hypoxia treatment can significantly elevate the beneficial effect of ADSC-Exos in the fat grafting. These findings are consistent with

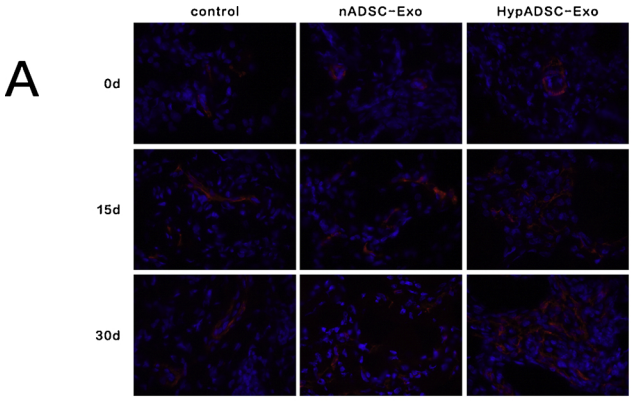

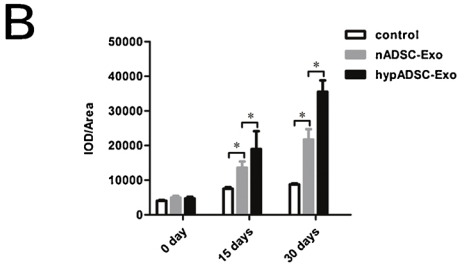

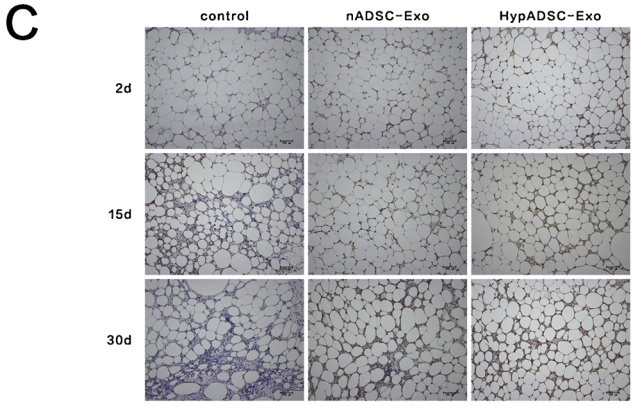

D

	1	2	3	4	1	2	3	4	1	2	3	4
A	POS1				POS2				NEG			
B	ANG-1				Angiostatin				CXCL16			
C	EGF				FGF-4				Follistatin			
D	G-CSF				GM-CSF				I-309			
E	IL-1b				IL-4				IL-10			
F	IL-12p40				IL-12p70				I-TAC			
G	MCP-2				MCP-3				MCP-4			
H	MMP-1				MMP-9				PECAM-1			
I	TGFα				TGFβ3				Tie-1			
J	Tie-2				uPAR				VEGF			
K	VEGF R2				VEGF R3				VEGF-D			

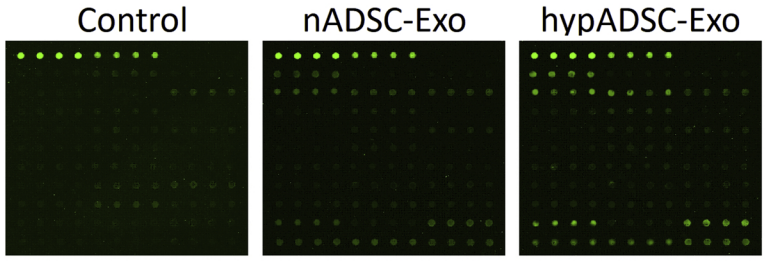

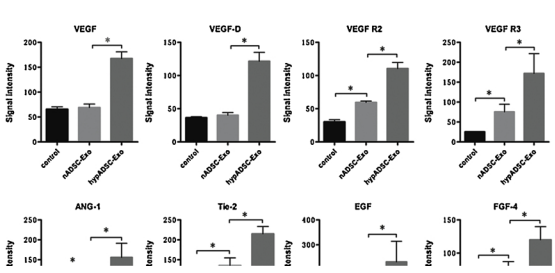

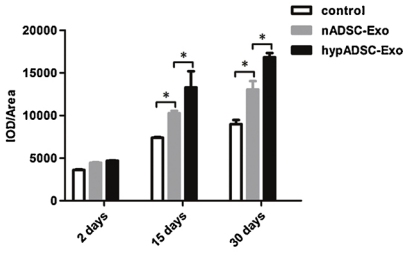

Fig. 6. The effect of nADSC-Exo and hypADSC-Exo on mice model of fat grafting. (A) nADSC-Exo and hypADSC-Exo promoted angiogenesis *in vivo*. CD31-marked vascular endothelial cells were observed in the fat graft sections immediately, and 15 days and 30 days after grafting. (B) Quantitative analysis of the intensity of fluorescent density (IOD). PBS-treatment was used as negative control (mean ± SEM, * $p < 0.05$, n = 3). (C) The images of the scanned protein array of three groups. The left table indicates the array map. Each antibody is printed in quadruplicate horizontally. (D) VEGF-R2 expression in the grafted fat sections was assessed using IHC analysis at 2 days, 15 days, and 30 days after nADSC-Exo, hypADSC-Exo, or PBS treatment. (E) The profile of proteins that differed between fat samples treated with nADSC-Exo or hypADSC-Exo. PBS-treatment was used as negative control (mean ± SEM, * $p < 0.05$, n = 2). (F) Quantitative analysis of the intensity of color density of IHC for VEGF-R2 (mean ± SEM, * $p < 0.05$, n = 3).

previous observations (Han et al., 2018). However, the current study further investigated the underlying mechanism. Given that the cargos carried by exosome are largely affected by the microenvironment (Hofmann et al., 2012), the enhanced pro-angiogenic potential of hypADSC-Exos may be attributed to the cargo in exosomes. Consequently, we adopted protein array to compare the levels of angiogenesis-related proteins between the ADSC-Exos from normoxia- and hypoxia-treated ADSCs. Our results showed that there was a significant enrichment of bFGF, VEGF/VEGF-R, and chemotactic factors (MCP-2, MCP-4) levels in the hypADSC-Exo than in the nADSC-Exo. All these proteins have been shown to promote vascular endothelial cells function (Su et al., 2017). Our NTA data showed that the particle size of hypADSC-Exo was larger than that of nADSC-Exo, which may create a higher cargo-carrying capacity and contribute to the enhanced pro-angiogenic potential of hypADSC-Exo.

Our animal study showed that the expressions of growth factors, such as ANG-1/Tie-2, EGF, bFGF VEGF/VEGF-R, were significantly up-regulated in the grafted tissue of hypADSC-Exo-treated mice. The IHC analysis also confirmed the elevated VEGF-R expression in grafted tissue. This phenomenon is likely attributed to the fact that the hypADSC-Exo delivered more growth factors to the recipient cells, which led to the elevated expression of VEGF-R in grafted tissue. VEGF/VEGF-R signaling is a well-studied angiogenic factor specific to endothelial cells (Abhinand et al., 2016). VEGF/VEGF-R signaling plays key roles in regulating the formation of new blood vessels, such as induction of gene expression, regulation of vascular permeability, and promotion of cell migration, proliferation and survival (Lee et al., 2007). These regulations are initiated by the binding of VEGF to VEGF-Rs, followed by activation of multiple downstream signaling pathways (Sullivan and Brekken, 2010). Hence, the high levels of VEGF/VEGF-R in the hypADSC-Exo may account for its high pro-angiogenic effect. These findings indicate that hypoxia preconditioning could be used as an efficient method to enrich pro-angiogenic factors in MSC-derived exosomes.

There are still some limitations in this study. Although we identified several key growth factors with differential levels between nADSC-Exo and hypADSC-Exo, we did not investigate if these proteins directly account for the proangiogenic potential of exosomes from hypoxia-treated human ADSCs. In addition, the downstream molecules in the signaling pathways remain to be identified. Furthermore, our protein array analysis only assessed 30 angiogenesis-related proteins. Characterizing the whole protein profile of nADSC-Exo and hypADSC-Exo should provide more details for the molecular mechanism. All these limitations should be addressed in the future study.

5. Conclusion

In summary, our findings suggested that exosomes derived from hypoxia preconditioned human ADSCs possess a higher capacity to enhance angiogenesis both *in vitro* and *in vivo*, at least partially, *via* VEGF/VEGF-R signaling. These findings may be helpful for developing a new strategy to improve the survival of fat grafts.

Declarations of interest

None.

Funding

This work was supported by the National Natural Science Foundation of China Grant [81571864].

Acknowledgment

None.

References

Abhinand, C.S., Raju, R., Soumya, S.J., Arya, P.S., Sudhakaran, P.R., 2016. VEGF-A/VEGFR2 signaling network in endothelial cells relevant to angiogenesis. J. Cell Commun. Signal. 10, 347–354.
Bang, C., Thum, T., 2012. Exosomes: new players in cell-cell communication. Int. J. Biochem. Cell Biol. 44, 2060–2064.
Chang, C.-P., Chio, C.-C., Cheong, C.-U., Chao, C.-M., Cheng, B.-C., Lin, M.-T., 2013. Hypoxic preconditioning enhances the therapeutic potential of the secretome from cultured human mesenchymal stem cells in experimental traumatic brain injury. Clin. Sci. (Lond.) 124, 165–176.
Cheung, A.L., 2007. Isolation and Culture of Human Umbilical Vein Endothelial Cells (HUVEC), in Current Protocols in Microbiology.
Coleman, S.R., Katzel, E.B., 2015. Fat grafting for facial filling and regeneration. Clin. Plast. Surg. 42, 289–300.
Comella, K., Parlo, M., Daly, R., Depasquale, V., Edgerton, E., Mallory, P., Schmidt, R., Drake, W.P., 2017. Safety analysis of autologous stem cell therapy in a variety of degenerative diseases and injuries using the stromal vascular fraction. J. Clin. Med. Res. 9, 935–942.
Condé-Green, A., Marano, A.A., Lee, E.S., Reisler, T., Price, L.A., Milner, S.M., Granick, M.S., 2016. Fat grafting and adipose-derived regenerative cells in burn wound healing and scarring: a systematic review of the literature. Plast. Reconstr. Surg. 137, 302–312.
Del Vecchio, D.A., Del Vecchio, S.J., 2014. The graft-to-capacity ratio: volumetric planning in large-volume fat transplantation. Plast. Reconstr. Surg. 133, 561–569.
Guo, S.-C., Tao, S.-C., Yin, W.-J., Qi, X., Yuan, T., Zhang, C.-Q., 2017. Exosomes derived from platelet-rich plasma promote the re-epithelization of chronic cutaneous wounds via activation of YAP in a diabetic rat model. Theranostics 7, 81–96.
Han, Y., Bai, Y., Yan, X.-L., Ren, J., Zeng, Q., Li, X.-D., Pei, X.-T., Han, Y., 2018. Co-transplantation of exosomes derived from hypoxia-preconditioned adipose mesenchymal stem cells promotes neovascularization and graft survival in fat grafting. Biochem. Biophys. Res. Commun. 497, 305–312.
Herold, C., Ueberreiter, K., Busche, M.N., Vogt, P.M., 2013. Autolog us fat transplantation: volumetric tools for estimation of volume survival. A systematic review. Aesthetic Plast. Surg. 37, 380–387.
Hofmann, N.A., Ortner, A., Jacamo, R.O., Reinisch, A., Schallmoser, K., Rohban, R., Etchart, N., Fruehwirth, M., Beham-Schmid, C., Andreeff, M., Strunk, D., 2012. Oxygen sensing mesenchymal progenitors promote neo-vasculogenesis in a humanized mouse model in vivo. PLoS One 7.
Hu, G., Li, Q., Niu, X., Hu, B., Liu, J., Zhou, S., Guo, S., Lang, H., Zhang, C., Wang, Y., Deng, Z., 2015. Exosomes secreted by human-induced pluripotent stem cell-derived mesenchymal stem cells attenuate limb ischemia by promoting angiogenesis in mice. Stem Cell Res. Ther. 6, 10.
Krämer-Albers, E.-M., Hill, A.F., 2016. Extracellular vesicles: interneural shuttles of complex messages. Curr. Opin. Neurobiol. 39, 101–107.
Lai, R.C., Yeo, R.W.Y., Lim, S.K., 2015. Mesenchymal stem cell exosomes. Semin. Cell Dev. Biol. 40, 82–88.
Lee, S., Chen, T.T., Barber, C.L., Jordan, M.C., Murdock, J., Desai, S., Ferrara, N., Nagy, A., Roos, K.P., Iruela-Arispe, M.L., 2007. Autocrine VEGF signaling is required for vascular homeostasis. Cell 130, 691–703.
Liu, X., Li, Q., Niu, X., Hu, B., Chen, S., Song, W., Ding, J., Zhang, C., Wang, Y., 2017. Exosomes secreted from human-induced pluripotent stem cell-derived mesenchymal stem cells prevent osteonecrosis of the femoral head by promoting angiogenesis. Int. J. Biol. Sci. 13, 232–244.
Madrigal, M., Rao, K.S., Riordan, N.H., 2014. A review of therapeutic effects of mesenchymal stem cell secretions and induction of secretory modification by different culture methods. J. Transl. Med. 12 (1), 260.
Majmundar, A.J., Wong, W.J., Simon, M.C., 2010. Hypoxia-inducible factors and the response to hypoxic stress. Mol. Cell 40, 294–309.
Merino-González, C., Zuñiga, F.A., Escudero, C., Ormazabal, V., Reyes, C., Nova-Lamperti, E., Salomón, C., Aguayo, C., 2016. Mesenchymal stem cell-derived extracellular vesicles promote angiogenesis: potencial clinical application. Front. Physiol. 7, 24.
Pankajakshan, D., Agrawal, D.K., 2014. Mesenchymal stem cell paracrine factors in vascular repair and regeneration. J. Biomed. Technol. Res. 1.
Pu, L.L.Q., 2016. Mechanisms of fat graft survival. Ann. Plast. Surg. 77, S84–S86.
Raposo, G., Stoorvogel, W., 2013. Extracellular vesicles: exosomes, microvesicles, and friends. J. Cell Biol. 200, 373–383.
Simonacci, F., Bertozzi, N., Grieco, M.P., Grignaffini, E., Raposio, E., 2016. Autologous fat transplantation for breast reconstruction: a literature review. Ann. Med. Surg. 12, 94–100.
Stillaert, F., Depypere, B., Doornaert, M., Creytens, D., De Clercq, H., Cornelissen, R., Monstrey, S., Blondeel, P., 2016. Autologous plasma and its supporting role in fat graft survival: a relevant vector to counteract resorption in lipofilling. J. Plast. Reconstr. Aesthet. Surg. 69, 952–958.
Su, S.-A., Xie, Y., Fu, Z., Wang, Y., Wang, J.-A., Xiang, M., 2017. Emerging role of exosome-mediated intercellular communication in vascular remodeling. Oncotarget 8, 25700–25712.
Suga, H., Glotzbach, J.P., Sorkin, M., Longaker, M.T., Gurtner, G.C., 2014. Paracrine mechanism of angiogenesis in adipose-derived stem cell transplantation. Ann. Plast. Surg. 72, 234–241.
Sullivan, L.A., Brekken, R.A., 2010. The VEGF family in cancer and antibody-based strategies for their inhibition. MAbs 2, 165–175.
Théry, C., Amigorena, S., Raposo, G., Clayton, A., 2006. Isolation and characterization of exosomes from cell culture supernatants and biological fluids. Curr. Protoc. Cell Biol

Chapter 3, Unit 3.22.
Tian, T., Zhu, Y.-L., Hu, F.-H., Wang, Y.-Y., Huang, N.-P., Xiao, Z.-D., 2013. Dynamics of exosome internalization and trafficking. J. Cell. Physiol. 228, 1487–1495.
Wetterau, M., Szpalski, C., Hazen, A., Warren, S.M., 2012. Autologous fat grafting and facial reconstruction. J. Craniofac. Surg. 23, 315–318.
Yoshimura, K., Sato, K., Aoi, N., Kurita, M., Hirohi, T., Harii, K., 2008a. Cell-assisted lipotransfer for cosmetic breast augmentation: supportive use of adipose-derived stem/stromal cells. Aesthetic Plast. Surg. 32 48–55–7.
Yoshimura, K., Sato, K., Aoi, N., Kurita, M., Inoue, K., Suga, H., Eto, H., Kato, H., Hirohi, T., Harii, K., 2008b. Cell-assisted lipotransfer for facial lipoatrophy: efficacy of clinical use of adipose-derived stem cells. Dermatol. Surg. 34, 1178–1185.
Zhang, H.-C.C., Liu, X.-B.B., Huang, S., Bi, X.-Y.Y., Wang, H.-X.X., Xie, L.-X.X., Wang, Y.-Q.Q., Cao, X.-F.F., Lv, J., Xiao, F.-J.J., Yang, Y., Guo, Z.-K.K., 2012. Microvesicles derived from human umbilical cord mesenchymal stem cells stimulated by hypoxia promote angiogenesis both in vitro and in vivo. Stem Cells Dev. 21, 3289–3297.
Zhao, J., Yi, C., Li, L., Zheng, Y., Wu, K., Liang, L., Xia, W., Guo, S., 2012. Observations on the survival and neovascularization of fat grafts interchanged between C57BL/6-gfp and C57BL/6 mice. Plast. Reconstr. Surg. 130.